Desalination and Water Treatment
www.deswater.com

doi: 10.1080/19443994.2014.886295

54 (2015) 699–706
April

Taylor & Francis
Taylor & Francis Group

Degradation of Reactive Red 3 by heterogeneous Fenton-like process over iron-containing RH-MCM-41 assisted by UV irradiation

K. Wantala[a,b,c,*], C. Khamjumphol[a,b], N. Thananukool[a,b], A. Neramittagapong[b,c]

[a]*Chemical Kinetics and Applied Catalysis Laboratory (CKCL), Khon Kaen University, Khon Kaen 40002, Thailand Tel. +664 336 2240x42; Fax: +664 336 2240; email: kitirote@kku.ac.th*
[b]*Faculty of Engineering, Department of Chemical Engineering, Khon Kaen University, Khon Kaen 40002, Thailand*
[c]*Faculty of Engineering, Research Center for Environmental and Hazardous Substance Management (EHSM), Khon Kaen University, Khon Kaen 40002, Thailand*

Received 24 August 2013; Accepted 16 January 2014

ABSTRACT

The degradation of Reactive Red 3 dye (RR3) by Photocatalytic Wet Peroxidation (PCWPO) on Fe-RH-MCM-41 (Si/Fe = 10) catalyst, a mesoporous molecular sieve prepared by direct hydrothermal technique was studied. Rice husk silica was used as silica precursor. The catalyst was investigated by X-ray diffraction, X-ray Fluorescence spectrophotometer, BET and UV-DRs techniques. The catalyst activity was designed by Box–Behnken design (BBD). The effects of initial pH of the solutions, initial H_2O_2 concentrations and reaction temperature in PCWPO process were investigated by BBD. The characterized results indicate a surface area of about 801 m^2/g and indicate that ferric was not detected on the surface of RH-MCM-41. Initial pH of dye solution and temperature of reaction were found to be significant on RR3 removal while initial concentration of H_2O_2 was found to be insignificant. The maximum condition was 48.375 mM for initial H_2O_2 concentration, 50°C for reaction temperature, and 3 for initial pH of the solution.

Keywords: Rice husk silica; Dye wastewater; *In situ* technique; PhotoFenton-like; Heterogeneous catalyst

1. Introduction

Untreated wastewater is harmful to humans, plants and animals. Many industries like small textile industries discharge wastewater to the environment without good wastewater management. Therefore, this wastewater is assumed to have bad impact on the environment. Dye wastewater is known to be persistent and cannot be treated by biological and physical processes only. As a result of the need to treat it, chemical process was applied to it in soluble form. In addition to this, advanced oxidation processes such as photocatalysis, electo-Fenton, wet air oxidation, and photoelectron-Fenton were studied by many researchers [1–15]. Kasiri and his co-worker [9] reported that Fenton process in homogenous catalyst condition give high activity to degrade organic pollutants. However, this process must be performed under low pH and the separation of homogenous catalyst after the reaction was difficult. To solve the catalyst separation process, many researchers became more interested in heterogeneous catalysts for Fenton process. Fe as one of the famous catalysts used in homogenous reaction was studied in this research. According to some

*Corresponding author.

research, Fe loaded on surface of some supports show high activity. However, it was observed that high concentration of Fe leached in the solution. To solve Fe leaching, substitution in the lattice of mesoporous materials was studied in this research similar to our previous work [16]. Yaman and co-worker [11] studied Fenton-like process by using iron-containing ZSM-5 zeolites to degrade CI Reactive Red 141 dye and also reported that the leached Fe was low (lower than 2 mg/l). Our previous research conditions which include pH 3, 6, and 9 and initial H_2O_2 concentrations $[H_2O_2]_0$ of 24.475, 48.950, and 73.425 mM, found that RR3 degradation was apparent only at pH 3. The degradation was found to be slightly increase when $[H_2O_2]_0$ was increased from 24.475 to 48.950 mM and then, it became stable at higher concentrations. Based on previous works [16], the optimum condition cannot be found except for maximal condition. However, we increased $[H_2O_2]_0$ and decreased pH of the solution. On the other hand, many researchers reported that ultraviolet irradiation (UV) can enhance dye degradation under Fenton reaction [6,10,15]. It can be concluded that the combination of Fenton reaction and UV light can give higher efficiency than Fenton process only.

The aims of this research were to synthesize heterogeneous catalyst by adding Fe into the lattice of mesoporous materials prepared from rice husk silica (Fe-RH-MCM-41) by hydrothermal technique and to investigate its performance to degrade RR3 in batch reactor using photocatalytic wet peroxidation process (PCWPO). The independent variables such as initial H_2O_2 concentration, pH of solution and reaction temperature were studied in terms of main, square, and interaction effects using Box–Behnken design (BBD) based on Response Surface Methodology (RSM). Compared to our previous work, different range of values was given to the said variables [16] to find the optimum condition.

2. Materials and methods

2.1. Chemicals

All chemicals were of analytical grade and were bought from Ajax Laboratory Chemical (Australia), Fluka (Spain), Riedal-Dehaen (Germany), Kanto Chemical (Japan), Acros Organics (USA) and J. T. Baker (USA). All of them were used as received. The RR3 dye was supplied from textile industry. The molecular formula of RR3 is $C_{25}H_{15}ClN_7Na_3O_{10}S_3$ with the formula weight of 774.04 g/mole. The structure of the RR3 is shown in Fig. 1 [16]. RR3 solution was prepared by dissolving it with distilled water.

2.2. Catalyst preparations

The Fe-RH-MCM-41 was prepared according to our previous work [16,17] (i) Hexadecyltrimethyl ammonium bromide (CTAB) of 4.50 g and Fe precursor were mixed with 90 ml of deionized water in a Teflon beaker, (ii) sodium silicate was prepared in another Teflon container by dissolving 5.00 g of NaOH in 30 ml of deionized water, then, 3.00 g of rice husk silica was added as obtained from Si/Fe mole ratio of 10. Next, the solution was stirred vigorously until it was clear and viscous. The CTAB alkali solution was poured into the prepared sodium silicate. The mixture was adjusted to make its pH about 11. Then, the gel was aged in the autoclave at 100˚C for 3 days. After aging, the suspended solids were filtered, and then washed with deionized water, then, dried in an oven overnight and calcined in the furnace at 550˚C for 6 h under airflow.

2.3. Catalyst characterizations

Structural characterization of the samples was carried out using X-ray diffraction (XRD) (Model D8 Discover, Bruker AXS, Germany) equipped with a Cu Kα radiation source (wavelength 1.514 Å). All of the powder samples were investigated at a scanning range of 1.5–15° with an increment of 0.02˚. X-ray Fluorescence spectrophotometer (XRF) was used to check the quantity of elements present in the sample and to confirm the Si/Fe molar ratio in Fe-RH-MCM-41. The surface area was analyzed by BET technique. UV-DR spectroscopy was carried out by SPECORD (AnalytikJena, Germany) under the wavelength range of 300–800 nm.

2.4. Test performance of Fe-RH-MCM-41 catalyst

The catalyst activity was separated in two parts. The first part aimed to confirm the performance of our catalysts by using many degradation processes (only

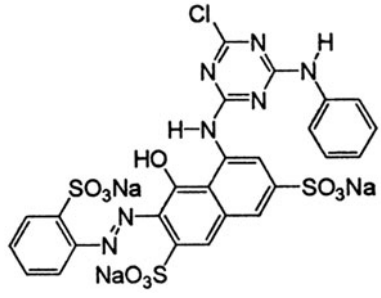

Fig. 1. Structure of the RR3.

UV, Fe-RH-MCM-41/UV, H_2O_2/UV, Fe-RH-MCM-41/H_2O_2, and Fe-RH-MCM-41/H_2O_2/UV). Two hundred milliliters of RR3 solution ($[RR3]_0 = 50$ mg/l) and about 0.2 g of catalyst in powdered form were loaded in the reactor. After the reaction mixture was magnetically stirred at about 15 min, the pH was then adjusted to 3 and the temperature was controlled at about 50˚C. After that, hydrogen peroxide ($[H_2O_2]_0 = 64.500$ mM) was added at once. The UV-C irradiated source was used from low-pressure mercury lamp (6 W). During all the oxidation reactions, samples were collected at 0, 5, 10, and 20 min and filtered by pore size 0.45 μm filter membrane. The reaction was then blocked by dropping 1.0 M of NaOH solution to adjust pH to 9–10. After that, remaining RR3 was analyzed by UV–visible spectroscopy at maximum adsorption wavelength (533 nm). The second part involved the use of BBD to investigate catalytic degradation parameters affecting RR3 removal using Fe-RH-MCM-41 catalyst. Studied variables were initial H_2O_2 concentrations (X_1), initial solution pH (X_2), and reaction temperature (°C) (X_3), whereas the output data was RR3 degradation (% removal; Y). The independent variables and levels of variables are shown in Table 1. The main differences of independent variables in this research as compared to our previous work [16] were ranges of pH of solutions and initial H_2O_2 concentrations. The solution pH were changed from 3, 6, and 9 to 3, 4, and 5 and the initial H_2O_2 concentrations were changed from 24.475, 48.950, and 73.425 mM to 48.375, 64.500, and 80.625 mM. Designed new ranges of independent variables were based on our previous work where the lowest pH and the highest initial H_2O_2 concentration were most favorable. The second part was done by the following, 200 ml of RR3 solution ($[RR3]_0 = 50$ mg/l) and about 1 g/l of Fe-RH-MCM-41 catalyst in powdered form were loaded in the reactor. After the reaction mixture was magnetically stirred at about 15 min. Then, the pH was adjusted and temperature was ccontrolled following run orders shown in Table 2. After that, hydrogen peroxide was added at once following run orders shown in Table 2, as well. The UV-C irradiated source was used from low-pressure mercury lamp (6 W). The reaction time was 10 min. After that, the samples were collected and filtered by a filter membrane with pore size of 0.45 μm. The reaction was then blocked by dropping 1.0 M of NaOH solution to adjust pH to 9–10. After that, remaining RR3 was analyzed by UV–visible spectroscopy at maximum adsorption wavelength (533 nm). The following formula was used to calculate the response value that was percent RR3 removal (Y) as shown in Eq. (1):

$$Y = \frac{C_0 - C_t}{C_0} \times 100 \quad (1)$$

where Y is RR3 removal (%), C_o and C_t are initial concentration and RR3 concentration after reaction time of 10 min (ppm), respectively.

Table 1
Independent variables and levels of factors used for optimization

Variable	Level		
	Low (−)	Middle (0)	High (+)
Initial H_2O_2 concentration (mM); X_1	48.375	64.500	80.625
pH; X_2	3	4	5
Temperature (°C); X_3	30	40	50

3. Results and discussion

3.1. Characterizations of Fe-RH-MCM-41

Fig. 2 shows the XRD patterns of Fe-RH-MCM-41 compared with rice husk silica (RH-SiO_2). The result showed the presence of major peak at about 2.3 (2˚θ) and minor peaks at about 3.9, 4.5, and 5.9 (2˚θ) same position as RH-MCM-41 [16,18]. According to results, we can conclude that Fe is inserted in the lattice of RH-MCM-41 and Fe-RH-MCM-41 was still shown in hexagonal array. It was also confirmed by XRF that the Si/Fe molar ratio was about 9.3 which was similar to the designed molar ratio (Si/Fe = 10). The surface area of Fe-RH-MCM-41 was calculated by BET technique and was found to be about 801 m^2/g. It was then compared to silica from rice husk with surface area of about 240 m^2/g [19]. It can be observed that the surface area of Fe-RH-MCM-41 was greater than 3.3 times the surface area of silica.

The characterizations of catalyst by using UV-DRs technique is shown in Fig. 3. The peak of Fe_2O_3 at 530 nm [20] was not found in the pattern of Fe-RH-MCM-4. It indicated that all Fe were inserted into the lattice of the mesoporous material by substitution with some Si atoms in the structure of MCM-41. Based on the characterized results, it was concluded that Fe-RH-MCM-41 was completely prepared by direct hydrothermal technique. Catalyst performance on PCWPO process was then tested.

3.2. Test performance of Fe-RH-MCM-41 catalyst

Fig. 4 shows RR3 degradation in several processes with Fe-RH-MCM-41. The Fe-RH-MCM-41 with UV

Table 2
Combinatorial optimization of the PCWPO degradation of RR3 for 10 min

Run order	H_2O_2 (mM)	pH	Temperature (°C)	Y%
1	80.625	5	40	3.894
2	48.375	5	40	3.476
3	64.500	5	30	4.089
4	64.500	5	50	4.060
5	64.500	4	40	6.622
6	64.500	3	30	96.171
7	48.375	4	50	29.000
8	64.500	3	50	95.786
9	64.500	5	50	5.605
10	64.500	4	40	3.747
11	48.375	3	40	95.489
12	80.625	5	40	2.153
13	48.375	4	30	5.070
14	48.375	5	40	7.870
15	80.625	4	30	3.208
16	80.625	4	30	2.119
17	64.500	4	40	8.869
18	80.625	3	40	97.257
19	80.625	3	40	96.441
20	80.625	4	50	8.435
21	48.375	4	50	13.857
22	64.500	4	40	9.175
23	64.500	3	50	96.823
24	64.500	4	40	4.349
25	64.500	4	40	4.824
26	64.500	3	30	95.292
27	48.375	3	40	97.045
28	48.375	4	30	1.573
29	80.625	4	50	17.407
30	64.500	5	30	1.402

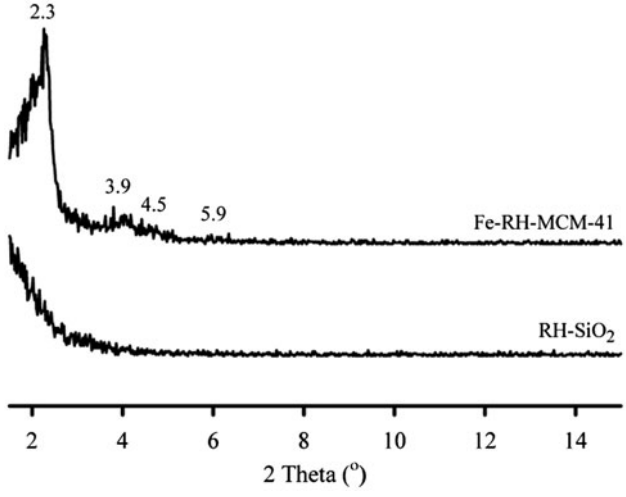

Fig. 2. XRD patterns of Fe-RH-MCM-41 compared with RH-SiO_2.

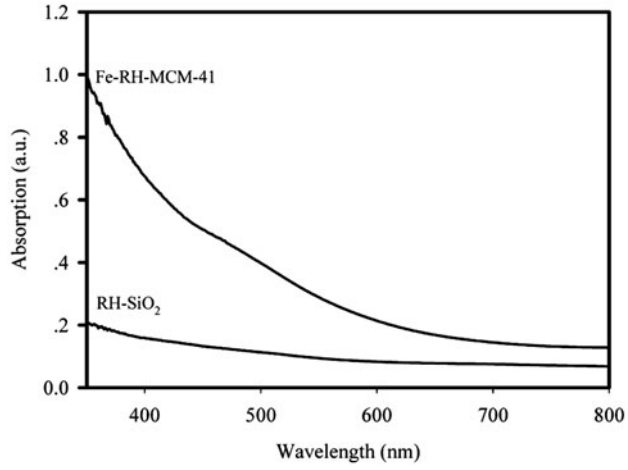

Fig. 3. UV-DRs patterns of Fe-RH-MCM-41 and RH-SiO_2.

light, only UV light, and H_2O_2 with UV light cannot degrade effectively while Fe-RH-MCM-41 and H_2O_2 with and without UV irradiation was able to outstandingly degrade almost 100% after the first 5 min. The UV irradiation with and without H_2O_2 processes, was found to be ineffective in the degradation, due to the low energy of UV lamp which is about 6 W, low pH (pH 3) [1] and short reaction times (20 min). The results show that Fenton reaction of catalytic wet peroxidation (CWPO, Fe-RH-MCM-41/H_2O_2) and photocatalytic wet peroxidation (PCWPO, -RH-MCM-41/H_2O_2/UV) processes were established by the RR3 degradation on Fe-RH-MCM-41 and H_2O_2 with and without light. However, PCWPO reaction was shown to be similar to CWPO reaction in terms of RR3 degradation. Low concentration of RR, low pH of solution, and reaction temperature at 50°C made the efficiency of RR3 degradation to be insignificantly different. Thus, PCWPO was selected over Fe-RH-MCM-41. Further investigation was done using Box–Behnken design based on RSM in high pH and $[H_2O_2]_0$ conditions to find the optimum conditions and interaction effects of these variables. Finally, the comparison of PCWPO and CWPO processes was investigated using higher pH.

The results of degradation activity of RR3 in PCWPO process for every condition designed by Box–Behnken method are shown in Table 2. The experimental results were calculated by Least Square of Error technique to find the regression quadratic equation or coefficient values as shown in Eq. (2).

$$Y = \beta_0 + \sum_{i=1}^{3} \beta_i X_i + \sum_{i=1}^{3} \beta_i^2 X_i^2 + \sum_{i=1}^{2} \sum_{j \neq i}^{3} \beta_{ij} X_i X_j \pm \varepsilon \qquad (2)$$

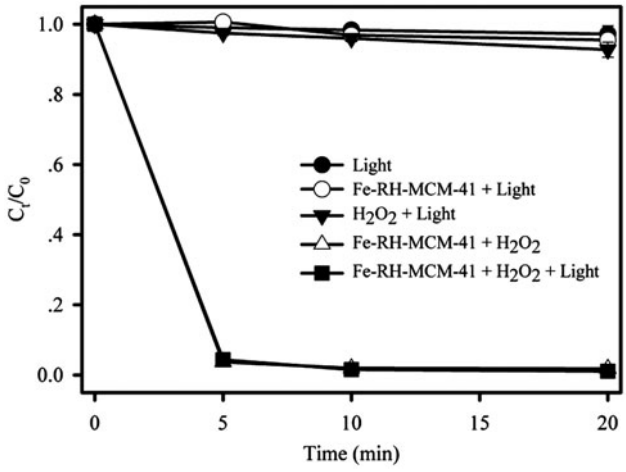

Fig. 4. Reactive Red 3 degradation in several processes. Reaction conditions: $[RR3]_0 = 50$ mg/l, Reactor volume = 200 ml, Fe-RH-MCM-41dose = 1 g/l, $[H_2O_2]_0 = 64.500$ mM, pH = 3.0, and T = 50°C.

where Y is the response (% removal of RR3), $\beta_0\beta_i\beta_i^2$ and β_{ij} are the constant coefficients, X is the coded independent variable (X_1, X_2, and X_3 are corresponding coded variables of $[H_2O_2]_0$, pH, and reaction temperature, respectively), and ε is the experimental error.

Table 3 shows the estimated regression coefficients of percentage of RR3 removal and p-values of the effects. At 95 percent confidence, pH and reaction temperature were found to have significant effect on RR 3 removal (p-value < 0.05). An approximate function of RR3 removal efficiency based on the experimental results was evaluated and given in Eq. 3. The obtained coefficient data are displayed in Table 3.

Table 3
Estimated regression coefficients (β) for % RR3 removal for 10 min

Variables	Coefficients	p-value
Constant	6.26	0.002
Initial H_2O_2 concentration (mM) (X_1)	−1.41	0.214
pH (X_2)	−46.11	0.000
Temperature (°C) (X_3)	3.87	0.002
Initial H_2O_2 concentration (mM) × initial H_2O_2 concentration (mM)	2.18	0.193
pH × pH	42.01	0.000
Temperature (°C) × temperature (°C)	1.63	0.325
Initial H_2O_2 concentration (mM) × pH	−0.81	0.609
Initial H_2O_2 concentration (mM) × temperature (°C)	−1.97	0.218
pH × temperature (°C)	0.38	0.810
$R^2 = 99.19\%$ $R^2(\text{adj}) = 98.83\%$		

$$Y = 6.26 - 1.41X_1 - 46.11X_2 + 3.87X_3 + 2.18X_1^2 + 42.01X_2^2 + 1.63X_3^2 - 0.81X_1X_2 - 1.97X_1X_3 + 0.3X_2X_3 \quad (3)$$

where Y is the predicted RR3 degradation (% removal), X_1, X_2, and X_3 are corresponding coded variables of $[H_2O_2]_0$, pH, and reaction temperature, respectively.

The diagnostic plots of this optimization study are shown in Fig. 5(a–d). The standard residuals calculated from predicted and experimental results show how well the model satisfies the assumptions of the analysis of variance (ANOVA) referring to our previous work [16,17,19,21]. The results are possibly due to the presence of a normal probability plot that was plotted approximately along a straight line as shown in Fig. 5(a). The histogram (Fig. 5(b)) shows the frequency of standard residuals shown in normal distributions. Fig. 5(c) presents random scatter plot of standard residuals vs. the fitted value presented as randomly scattered around the zero line. Fig. 5(d) exhibits the standard residuals vs. observation order results, which should oscillate in a random pattern around the zero line. According to these results, we concluded that all the experimental orders have no significant error.

A good agreement was obtained between the predicted RR3 removal and the actual experimental values. R^2 and R^2_{adj} were 99.19 and 98.83%, respectively, which indicated that the proposed model showed adequate approximation of the main variable effect on RR3 removal with a difference of only 0.36%. In addition, preliminary data also indicated the significance of each variable (X_1, X_2, and X_3) at 95% confidence interval. The p-values of the effect of initial pH of the solution and reaction temperature were less than 0.05 (Table 3) and the F-values of initial pH of the solution and reaction temperature were about 1764.00 and 12.64, respectively which were more than F-critical ($F_{(0.05,3,17)} = 3.20$). This showed that the initial pH of the solution and reaction temperature were significant in the degradation of RR3 while $[H_2O_2]_0$ was not significant (p-value equal to 0.214). The pH was observed to have the highest effect on RR3 removal. However, negative effect was observed, which means that an increase in pH would mean a decrease in RR3 removal. On the contrary, reaction temperature was found to have positive effect which indicated that degradation efficiency increased with increasing temperature. This can be explained by the increase in the

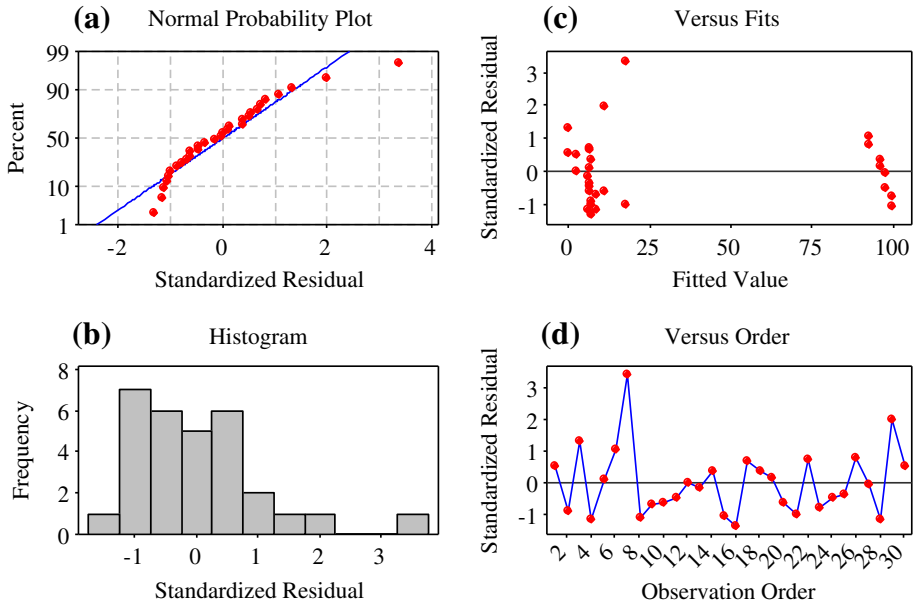

Fig. 5. Internal standard residual plots vs. normal probability, histogram, fits, and order.

reaction rate between hydrogen peroxide and ferric in the structure of Fe-RH-MCM-41. Thus, an increase in the rate of generation of oxidizing species such as $^{\bullet}OH$ radical caused the reactions between $^{\bullet}OH$ radical and RR3 and intermediate species to continue to mineralization process [3]. The *F*-value for the lack of fit was 4.82 which implied that the error of this model is insignificant (at 99% confidence, *F*-critical = 5.19). Thus, the model can be used to estimate the percent RR3 removal with (Eq. 3). Interaction effects of these variables are insignificant, referred by *F*-value < *F*-critical and *p*-value > 0.05, so, independent variables of this research such as $[H_2O_2]_0$, pH, and temperature have no relationship with each other.

The results in Figs. 6 and 7 showed that percent of RR3 removal increased with a decrease in pH and an increase in temperature. The percent removals of RR3 are nearly stable for all initial H_2O_2 concentrations. However, at high temperature and high initial H_2O_2 concentration, lower performance was observed as compared to low initial H_2O_2 concentration (less than 70 mM) as shown in Fig. 7(b). In addition to this, high temperature condition caused easier decomposition of H_2O_2 to form a combination of hydroxyl radicals, resulting to the decrease in degradation of dyes. It can be further explained by Eqs. (4)–(5) called recombination of hydroxyl radical.

$$^{\bullet}OH + H_2O_2 \rightarrow {}^{\bullet}O_2H + H_2O \quad (4)$$

$$^{\bullet}O_2H + {}^{\bullet}OH \rightarrow H_2O + O_2 \quad (5)$$

In Fig. 7, the results also confirmed that the interaction effects between initial pH of solution and $[H_2O_2]_0$ and initial pH of solution and reaction temperature were insignificant. However, in Fig. 7(a) and (c), there was no significant effect of $[H_2O_2)_0$ at all initial concentrations and reaction temperature at about 30 to 50°C on RR3 degradation efficiency at a specific value of solution pH. It was concluded that the efficiency of RR3 removal done at solution pH lower than 3.8 was dependent only on initial pH of the solution in all of $[H_2O_2]_0$ and reaction temperatures.

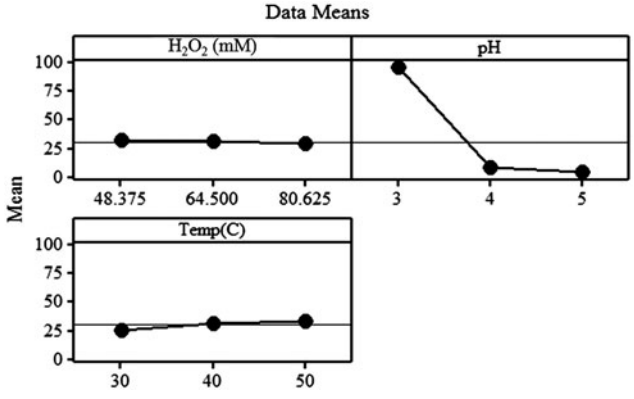

Fig. 6. Main effects plot for percent RR3 removal.

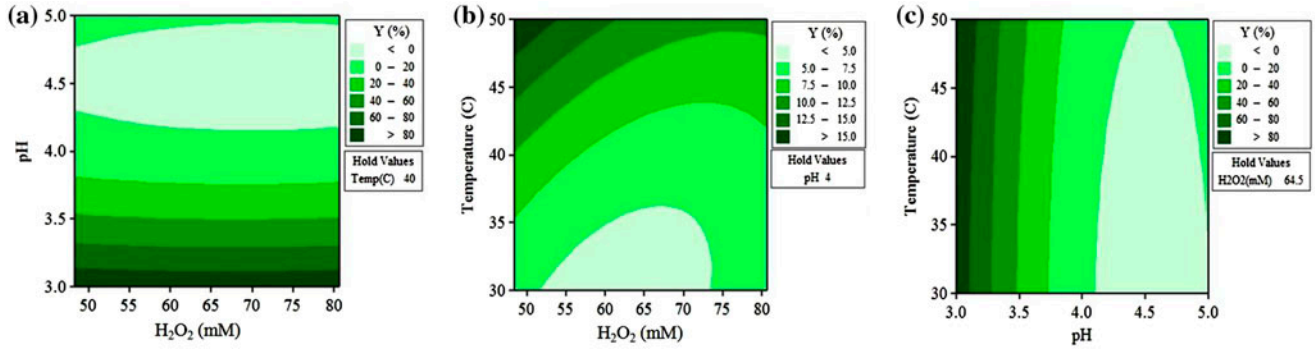

Fig. 7. Contour plots for removal percentage of RR3 for 10 min.

Eq. (3) can be used to predict the optimum condition for the degradation of RR3 obtained at 50˚C, pH 3 of the solution and 48.375 mM of $[H_2O_2]_0$. The maximal condition obtained from this research was obviously close to the one obtained by our previous work except for $[H_2O_2]_0$ shown at low concentration [16]. We are concerned about leaching of Fe to the solution, therefore, we measured the amount of leached Fe of the catalyst at the maximal condition and did not just observe it in the solution. It can be confirmed that the reaction took place on the surface of heterogeneous catalyst and adding Fe into the structure of RH-MCM-41 can prohibit the leach of Fe to the solution.

Finally, the comparison of the degradation efficiency between PCWPO and CWPO process was investigated. Fig. 8 shows the results of percent RR3 degradation between PCWPO and CWPO. It was found that at low pH (pH 3), RR3 degradation was quite similar for both processes at 30 and 50˚C. However, higher percent RR3 removal by PCWPO was observed at pH 4 and 5, especially at high temperature. It may be due to the reason that at high temperature (50˚C), H_2O_2 was activated to hydroxyl radical ($^{\bullet}OH$) reached with RR3. Feng and co-workers [10] reported the higher degradation of orange II under UV irradiation than without irradiation. One explanation of the increase in efficiency was that more hydroxyl radicals ($^{\bullet}OH$) were generated by direct photoreduction of $Fe(OH)^{2+}$ to react with the pollutants. Thus, it can be concluded that photoreduction can enhance the $^{\bullet}OH$ production resulting in enhanced RR3 degradation.

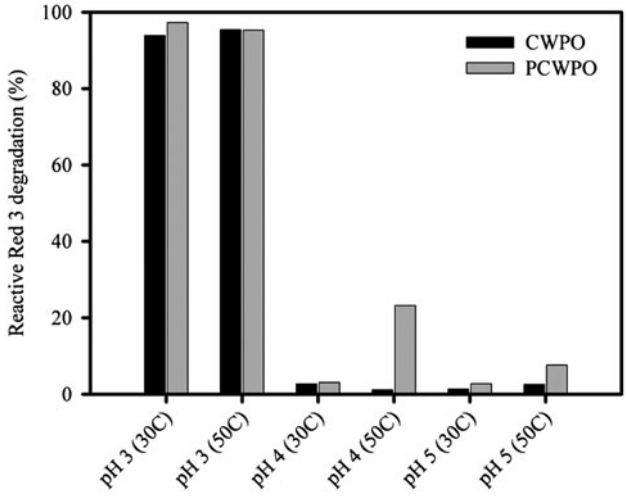

Fig. 8. Comparison of efficient degradation between PCWPO and CWPO. Reaction conditions: $[RR3]_0 = 50$ mg/l, Reactor volume = 200 ml, Fe-RH-MCM-41dose = 1 g/l, and $[H_2O_2]_0 = 48.375$ mM.

4. Conclusions

RR3 was degraded by photocatalytic wet peroxide oxidation (PCWPO) over Fe-RH-MCM-41. pH and reaction temperature were found to have significant effects on the percent RR3 removals while $[H_2O_2]_0$ was found to have insignificant effect on the degradation of RR3 dyes. The optimum conditions include reaction temperature of 50˚C, initial pH of solution equal to 3, and initial hydrogen peroxide concentrations of 48.375 mM. The PCWPO was confirmed to have higher degradation efficiency than CWPO at pH 4 and 5 and high temperatures by comparison test at the same condition.

Acknowledgments

The authors express their thanks to the Faculty of Engineering, Khon Kaen University and the Thailand Research Fund (TRF) for their strong support throughout this project and to Jessa Marie J. Millanar for language editing.

References

[1] I.A. Alaton, I.A. Balcioglu, D.W. Bahnemann, Advanced oxidation of a reactive dyebath effluent: Comparison of O_3, H_2O_2/UV-C and TiO_2/UV-A processes, Water Res. 36 (2002) 1143–1154.

[2] E.G. Garrido-Ramírez, B.K.G. Theng, M.L. Mora, Clays and oxide minerals as catalysts and nanocatalysts in Fenton-like reactions – A review, Appl. Clay Sci. 47 (2010) 182–192.

[3] N.K. Daud, U.G. Akpan, B.H. Hameed, Decolorization of Sunzol Black DN conc. in aqueous solution by Fenton oxidation process: effect of system parameters and kinetic study, Desalin. Water Treat. 37 (2012) 1–7.

[4] S.R. Patil, U.G. Akpan, B.H. Hameed, S.K. Samdarshi, A comparative study of the photocatalytic efficiency of Degussa P25, Qualigens, and Hombikat UV-100 in the degradation kinetic of congo red dye, Desalin. Water Treat. 46 (2012) 188–195.

[5] G. Calleja, J.A. Melero, F. Martínez, R. Molina, Activity and resistance of iron-containing amorphous, zeolitic and mesostructured materials for wet peroxide oxidation of phenol, Water Res. 39 (2005) 1741–1750.

[6] H. Kusic, N. Koprivanac, L. Srsan, Azo dye degradation using Fenton type processes assisted by UV irradiation: A kinetic study, J. Photochem. Photobiol. 181 (2006) 195–202.

[7] M. Dükkanci, G. Gündüz, S. Yilmaz, Y.C. Yaman, R.V. Prikhod'ko, I.V. Stolyarova, Characterization and catalytic activity of CuFeZSM-5 catalysts for oxidative degradation of Rhodamine 6G in aqueous solutions, Appl. Catal. B Environ. 95 (2010) 270–278.

[8] A.N. Soon, B.H. Hameed, Degradation of Acid Blue 29 in visible light radiation using iron modified mesoporous silica as heterogeneous Photo-Fenton catalyst, Appl. Catal. Gen. 450 (2013) 96–105.

[9] M.B. Kasiri, H. Aleboyeh, A. Aleboyeh, Degradation of Acid Blue 74 using Fe-ZSM5 zeolite as a heterogeneous photo-Fenton catalyst, Appl. Catal. B Environ. 84 (2008) 9–15.

[10] J. Feng, X. Hu, P.L. Yue, H.Y. Zhu, G.Q. Lu, Degradation of Azo-dye Orange II by a photoassisted fenton reaction using a novel composite of iron oxide and silicate nanoparticles as a catalyst, Ind. Eng. Chem. Res. 42 (2003) 2058–2066.

[11] Y.C. Yaman, G. Gündüz, M. Dükkancı, Degradation of CI Reactive Red 141 by heterogeneous Fenton-like process over iron-containing ZSM-5 zeolites, Color. Technol. 129 (2013) 69–75.

[12] J. Herney-Ramirez, M. Lampinen, M.A. Vicente, C.A. Costa, L.M. Madeira, Experimental design to optimize the oxidation of orange II dye solution using a clay-based fenton-like catalyst, Ind. Eng. Chem. Res. 47 (2008) 284–294.

[13] J.H. Ramirez, C.A. Costa, L.M. Madeira, G. Mata, M.A. Vicente, M.L. Rojas-Cervantes, A.J. López-Peinado, R.M. Martín-Aranda, Fenton-like oxidation of Orange II solutions using heterogeneous catalysts based on saponite clay, Appl. Catal., B 71 (2007) 44–56.

[14] S. Navalon, M. Alvaro, H. Garcia, Heterogeneous Fenton catalysts based on clays, silicas and zeolites, Appl. Catal., B 99 (2010) 1–26.

[15] H. Zheng, Y. Pan, X. Xiang, Oxidation of acidic dye Eosin Y by the solar photo-Fenton processes, J. Hazard. Mater. 141 (2007) 457–464.

[16] K. Wantala, P. Sriprom, N. Pojananukij, A. Neramittagapong, S. Neramittagapong, P. Kasemsiri, Optimal decolorization efficiency of reactive red 3 by Fe-RH-MCM-41 catalytic wet oxidation coupled with Box-Behnken design, Key Eng. Mater. 545 (2013) 109–114.

[17] K. Wantala, E. Khongkasem, N. Khlongkarnpanich, S. Sthiannopkao, K.-W. Kim, Optimization of As(V) adsorption on Fe-RH-MCM-41-immobilized GAC using Box–Behnken design: Effects of pH, loadings, and initial concentrations, Appl. Geochem. 27 (2012) 1027–1034.

[18] K. Wantala, S. Sthiannopkao, B. Srinameb, N. Grisdanurak, K.-W. Kim, S. Han, Arsenic adsorption by Fe loaded on RH-MCM-41 synthesized from rice husk silica, J. Environ. Eng. 138 (2012) 119–128.

[19] P. Tantriratna, W. Wirojanagud, S. Neramittagapong, K. Wantala, N. Grisdanurak, Optimization for UV-photocatalytic degradation of paraquat over titanium dioxide supported on rice husk silica using Box-Behnken design, Indian J. Chem. Technol. 18 (2011) 363–371.

[20] B. Li, K. Wu, T. Yuan, C. Han, J. Xu, X. Pang, Synthesis, characterization and catalytic performance of high iron content mesoporous Fe-MCM-41, Microporous Mesoporous Mater. 151 (2012) 277–281.

[21] D. Tipayarom, K. Wantala, N. Grisdanurak, Optimization of alachlor degradation on S-Doped TiO2by sonophotocatalytic activity under visible light, Fresenius Environ. Bull. 20 (2011) 1425–1431.